

MODELLING DOMAIN-AVERAGED SOLAR FLUXES FOR AN EVOLVING TROPICAL CLOUD SYSTEM

H.W. Barker¹ and Qiang Fu²

¹*Cloud Physics Research Division, Atmospheric Environment Service, Canada*

²*Atmospheric Science Program, Department of Oceanography, Dalhousie University, Canada*

Received December 8, 1998

Accepted February 1, 1999

Domain-averaged, broadband solar radiative budgets for an evolving tropical mesoscale convective cloud system are computed by two approximate 1D models which make different assumptions about the structure of unresolved clouds. One model is the standard plane-parallel, homogeneous (PPH) two-stream approximation. The other assumes that fluctuations in cloud extinction β can be described by a gamma distribution $p_{\Gamma}(\beta)$ and so weights the two-stream equations by $p_{\Gamma}(\beta)$ and integrates over all β . A 3D Monte Carlo (MC) algorithm provides reference calculations. The cloud system was simulated by a 2D cloud-resolving model and the domain measures 514 km horizontally and ~18 km vertically. Horizontal grid-spacing is 1 km while the 35 layers vary in thickness. The hydrometeors accounted for are liquid droplets, ice crystals, rain, graupel, and snow. Snapshots of the domain were saved every 5 model-minutes for 10 hours thus spanning the life-cycle of the system. It is shown that the conventional PPH two-stream is thoroughly inappropriate as it yields 10 hour mean TOA albedo α_{toa} and surface absorptance α_{sfc} of 0.56 and 0.20 but the corresponding 3D MC values are 0.32 and 0.47. For the gamma-weighted two-stream approximation (GWTS), however, α_{toa} and α_{sfc} are 0.32 and 0.49. Moreover, while heating rate errors for the PPH model are about -0.5 K/day near the surface and almost +2 K/day at 10 km, they are diminished at both altitudes to 0.25 K/day for the GWTS. For reference, it is shown that the independent column approximation is almost identical to the 3D MC and that while the best possible PPH model (i.e., perfect account of cloud overlap) is vastly superior to the regular PPH model, it is significantly inferior to the GWTS.

1. INTRODUCTION

At this stage, it is well known that neglect of cloud fluctuations at scales less than 10 km can seriously bias model estimates of the disposition of solar radiation in the Earth-atmosphere system.^{4,6,18} Since large-scale models (LSMs) of the atmosphere leave many cloud fluctuations unresolved, they require parametrizations of subgrid-scale clouds and their interaction with radiation. One such parametrization proposed by Barker² hypothesizes that if horizontal fluctuations in cloud optical depth τ can be approximated, even roughly, by a gamma distribution $p_{\Gamma}(\tau)$, then weighting the standard two-stream solutions by $p_{\Gamma}(\tau)$ and averaging should yield accurate estimates of both cloud albedo and transmittance. For a variety of cloud types, Barker et

al.³ and Oreopoulos and Barker¹⁵ demonstrated that this seems often to be the case. The purpose of this paper is to demonstrate the utility of this approximation using data spanning almost the entire life of a complex tropical convective cloud system. The following section describes briefly the models and data used in this study. Results are presented in the third section followed by concluding remarks.

2. DATA AND MODELS

2.1. Cloud-resolving model data and optical properties

The tropical cloud system used here was simulated by a 2D cloud-resolving model (CRM) forced by observations made during phase III of GATE with an underlying ocean.¹⁰ The domain measures 514 km

horizontally and ~18 km vertically. Horizontal grid-spacing is 1 km while the 35 layers vary in thickness from ~45 m at the surface to ~1 km at the top. The model was run with cyclic horizontal boundary conditions. Hydrometeors were categorized as: liquid droplets, ice crystals, rain, graupel, and snow. Optical properties of droplets, rain, graupel, and snow are based on Mie scattering theory⁹ while those for ice crystals are based on Fu hexagonal model.¹⁰ Rayleigh scattering is also considered and the surface is assumed to be black (to highlight cloud effects). Gaseous absorption coefficients for water vapour and O₃ (the latter following McClatchey et al. tropical profile¹⁴) are computed by the correlated-*k* distribution method (Ref. 8).

Snapshots of the domain were saved every 5 model-minutes for 12 hours thus spanning the tropical squall line's life-cycle. Only the last 10 hours are used as the first two lacked clouds and all mixing ratios less than 10⁻⁵ g/g are set to zero.

2.2. Radiative transfer models

Benchmark fluxes and heating rates are computed by a 3D Monte Carlo (MC) photon transport algorithm,^{1,11} using effective optical properties which are obtained by merging the gaseous and cloud optical properties thus yielding, for each cell, 54 effective monochromatic values of optical depth τ , single-scattering albedo ω_0 , and asymmetry parameter g . Cyclic horizontal boundary conditions are employed and to save MC CPU time, the original effective optical properties are transformed (see Joseph et al., 1976) as

$$\begin{aligned}\tau' &\leftarrow (1 - \omega_0 g^2)\tau, \\ \omega_0' &\leftarrow \frac{\omega_0(1 - g^2)}{1 - \omega_0 g^2}, \\ g' &\leftarrow \frac{g}{1 + g}.\end{aligned}\quad (1)$$

For many cases considered here, this reduces CPU usage by ~30% relative to when τ , ω_0 , and g are used (fewer scattering events) with minimal error. Iterating the mapping in Eq. (1) *ad infinitum*, the isotropic scattering approximation, reduces CPU usage even more, but flux errors can exceed 5% for very cloudy atmospheres with large solar zenith angles. For each of the 120 snapshots, 10⁶ photons were used. This leads to errors in domain-averaged TOA albedo α_{toa} and surface absorptance α_{sfc} of < 0.0005 and heating rate errors of typically < 1.5% per layer. The Henyey-Greenstein phase function¹² is used to describe scattering patterns. For all experiments, effective radius of liquid droplets is assumed to be 10 μm while for ice crystals it is 50 μm .

The standard plane-parallel homogeneous (PPH) two-stream approximation is used to represent, a near

outer envelope on, solar fluxes that an LSM would predict if provided with correct profiles of cloud fraction and mean cloud water mixing ratios. Layer values of reflectance and transmittance are computed as

$$\begin{aligned}R_{\text{pph}} &= (1 - C) R_{\text{clr}} + CR_{\text{clid}}(\bar{\tau}, \bar{\omega}_0, \bar{g}), \\ T_{\text{pph}} &= (1 - C) T_{\text{clr}} + CT_{\text{clid}}(\bar{\tau}, \bar{\omega}_0, \bar{g}),\end{aligned}\quad (2)$$

where R_{clr} and T_{clr} are for cloudless skies, R_{clid} and T_{clid} are two-stream solutions for the cloudy portion of a layer, and C is layer cloud fraction which is defined as

$$C \equiv \frac{\sum_{i=1}^{514} \Phi \left[\sum_{m=1}^5 L_m(i) \right]}{514} \leq \frac{\sum_{i=1}^{514} \left\{ \sum_{m=1}^5 \Phi[L_m(i)] \right\}}{514}, \quad (3a)$$

where

$$\Phi[L] \equiv \begin{cases} 1; & L > 0 \\ 0; & L = 0, \end{cases} \quad (3b)$$

and $L_m(i)$ is water path (g m^{-2}) of the m th condensate in the i th cell. The mean optical properties $\bar{\tau}$, $\bar{\omega}_0$, and \bar{g} for the cloudy portion of a layer are defined by first spreading all condensates over the cloudy region and defining mean water paths as

$$\bar{L}_m = \frac{\sum_{i=1}^{514} \Phi[L_m(i)] L_m(i)}{\sum_{i=1}^{514} \Phi \left[\sum_{m=1}^5 L_m(i) \right]}. \quad (4)$$

Then, optical properties $\tau(m)$, $\omega_0(m)$, and $g(m)$ for all 5 condensates are computed as well as those for Rayleigh scattering ($m = 6$), water vapor ($m = 7$), and O₃ ($m = 8$). Finally, they are averaged as

$$\begin{aligned}\bar{\tau} &= \sum_m \tau(m), \\ \bar{\omega}_0 &= \sum_m \omega_0(m) \tau(m) / \bar{\tau}, \\ \bar{g} &= \sum_m g(m) \omega_0(m) \tau(m) / \bar{\omega}_0 \bar{\tau}.\end{aligned}\quad (5)$$

The same is done for the clear-sky portions where it is clear that $\bar{L}_m = 0$ for all m . Hence, for the 1D models, only two sets of optical properties are computed (clear and cloudy; $2 \times 35 = 70$ cells), whereas for the MC they must be computed for all 17990 (= 514×35) cells. Once direct- and diffuse-beam reflectances and transmittances have been computed for each layer, linking proceeds following the principles of invariance as described by Liou.¹³

The GWTSa is the same as the PPH model except layer values are computed as

$$R_{\Gamma} = (1 - C) R_{\text{clr}} + C \int_0^{\infty} p_{\Gamma}(\bar{\tau}, \nu) R_{\text{clr}}(\tau, \bar{\omega}_0, \bar{g}) d\tau ,$$

$$T_{\Gamma} = (1 - C) T_{\text{clr}} + C \int_0^{\infty} p_{\Gamma}(\bar{\tau}, \nu) T_{\text{clr}}(\tau, \bar{\omega}_0, \bar{g}) d\tau , \quad (6)$$

where $p_{\Gamma}(\bar{\tau}, \nu)$ is the gamma distribution² in which ν is the solution to

$$\frac{d}{d\nu} \ln \Gamma(\nu) + \ln \left(\frac{\bar{L}_{\Sigma}}{\nu} \right) - \overline{\ln L_{\Sigma}} = 0 , \quad (7a)$$

where

$$L_{\Sigma} = \sum_{m=1}^5 L_m , \quad (7b)$$

is total water path in each cell. In addition, when clouds occur in contiguous layers, $\bar{\tau}$ are reduced for layers beneath the uppermost layer. This is a countervailing measure that partially remedies the use of mean (i.e., homogeneous) fluxes in the adding process. It is also worth mentioning that an empirical approach is taken to counter the implicit assumption of random overlapping cloud. For details regarding these approximations and closed-form expressions for the integrals in Eq. (6), see Ref. 15.

Both 1D codes employ Zdunkowski et al. Practical Improved Flux Method¹⁷ which does not yield negative fluxes for strong absorbing bands; a condition that sometimes plagues the more popular delta-Eddington (see Joseph et al., 1976).

Results from two other models are presented for reference. The independent column approximation (ICA) takes the full CRM fields, applies the regular 1D PPH model to each of the 514 columns, and averages the results. With the second model, cloud mixing ratios are first averaged and homogenized across each layer, as in Eq. (4), though cloud position is unaltered. Then, like the ICA, the 1D PPH model is applied to each column and the results are averaged. This model is referred to as PPH (perfect) since cloud overlap is accounted for perfectly but clouds are nevertheless PPH within each layer. It seems reasonable to think of this as the best possible 1D PPH model.

3. RESULTS

To begin, Fig. 1 summarizes some key radiative properties of the CRM simulation in the form of time-height plots of domain average profiles. The top panel shows cloud fraction and that clouds begin as an extensive deck between 1 km and 2 km which dissipates rapidly as vertical development proceeds. At about 0900 LAT, the anvil is well developed and eventually covers about 50% of the domain near 12 km at 1000. A second mass of convection begins at 1100 but is less vigorous than the initial blast and thus feeds the anvil only slightly. By 1600, the only significant cloud left is the thinning anvil whose extent at 10 km is about 35%. Figure 2 shows the 10 hour mean cloud fraction profile with the characteristic anvil maximum. This plot differs from Fig. 9 (of Ref. 10) as they averaged over the entire 12 hours and did not include the precipitation fields.

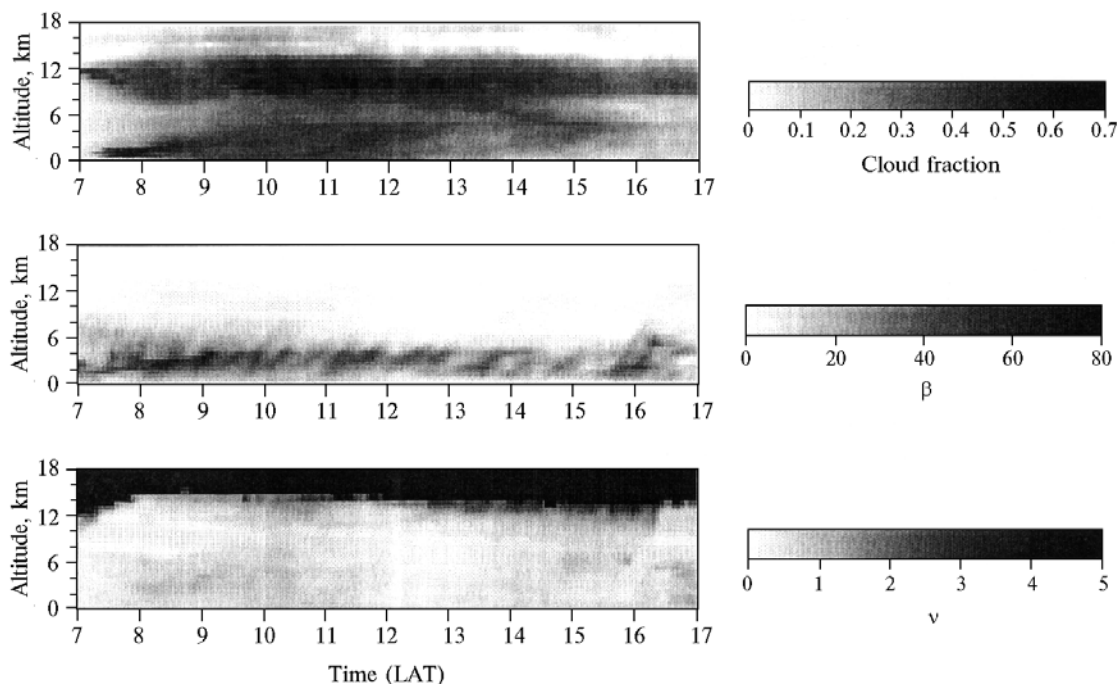


FIG. 1. Time-height plots of domain-average profiles of cloud fraction, cloud extinction coefficient β (km^{-1}), and ν as defined in Eq. (7a).

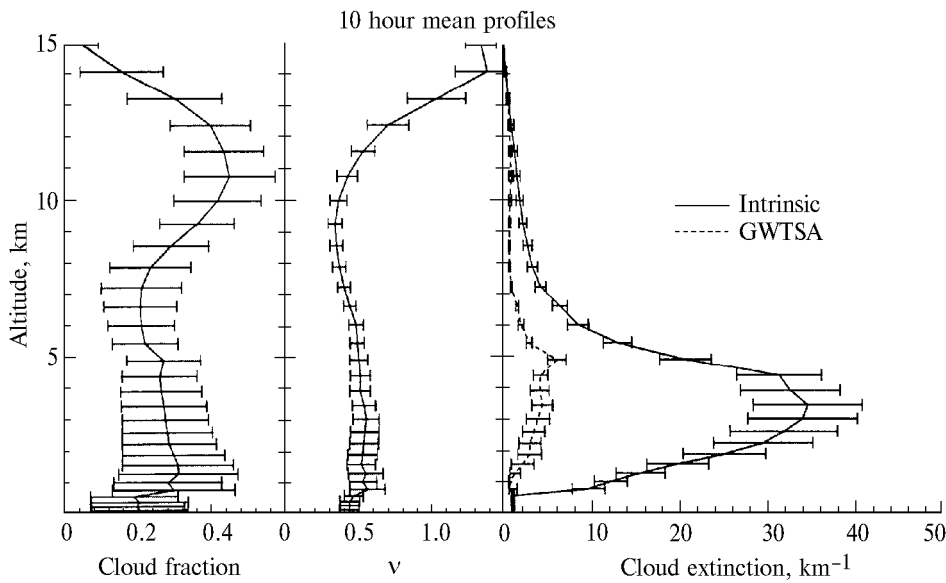


FIG. 2. Ten-hour mean, domain-averaged profiles of cloud fraction C and v as defined in Eq. (7a), as well as cloud extinction coefficient (km^{-1}) as used by the PPH and MC (intrinsic) and GWTSA models. Horizontal bars represent ± 1 standard deviation. With the exception of C , all data are weighted by cloud fraction.

Waves of convective growth are evident in Fig. 1's plot of cloud extinction (visible). Typically, significant cloud growth extends from 3 km to 5 km over the course of 30 minutes. Occasionally, mean β exceeds 50 km^{-1} at about 4 km whereas above the freezing level near 4.5 km, it rarely exceeds 20 km^{-1} . This transition from optically dense droplets to weakly attenuating ice, snow, and graupel can be seen clearly in Fig. 2 which shows mean profiles over the entire 10 hour period: near 4 km, mean β is typically $\sim 32 \text{ km}^{-1}$ but decreases to 8 km^{-1} by 6 km.

The final panel in Fig. 1 shows v as defined in Eq. (7a). For the most part, $v < 1$; only near the very tenuous cloudtops does v exceed 1 systematically. In fact, from the surface to 12 km, v is consistently ~ 0.5 (see Fig. 2). When the precipitation fields are neglected, v increases to typically 1.0. The impact of having such small values of v is evident in the rightmost panel of Fig. 2 which shows 10 hour mean profiles of intrinsic β and reduced β ; the latter being that which is operated on by the GWTSA (as alluded to in the previous section). Above 12 km, both intrinsic β and reduced β are almost equal, but below 5 km, β used by the GWTSA is roughly an order of magnitude less than the intrinsic values! Had the GWTSA used the intrinsic values of β , results would have been disastrous.

Radiative transfer calculations are for a site at the equator on July 15. To maximize the use of data, the middle of the 10 hour series was ascribed to solar noon. As such, the simulation begins at 0700 and ends at 1700 when the cosine of solar zenith angle μ_0 is ~ 0.25 . Furthermore, the 2D field is aligned from east-to-west. Thus, at sunrise, the Sun shines along the direction of

variability from 0 km to 514 km; at noon it has swings around to shine perpendicular to the direction of variability at a zenith angle of 21° , and at sunset it is again aligned parallel with the resolved variability but shines from 514 km to 0 km. Clouds are sheared towards the west.

Figure 3 shows time series of top of atmosphere (TOA) albedo α_{toa} , surface α_{sfc} and atmospheric absorptance α_{atm} for all five models considered here, and μ_0 . The fact that the ICA and full 3D MC simulations are essentially equal demonstrates that when only mean fluxes over large domains are of interest, details regarding cloud geometry are extraneous.⁴ This conclusion is reinforced by the 10 hour mean, domain-average values listed in Table I.

TABLE I. Ten hour mean TOA albedo (α_{toa}), surface absorptance (α_{sfc}), and atmospheric absorptance (α_{atm}) for the five models considered here (i.e., mean values of curves in Fig. 3 weighted by μ_0). Errors on the MC values are less than 0.01% of the values listed.

	3D	ICA	GW TSA	PPH (perfect)	PPH
α_{toa}	0.321	0.326	0.317	0.393	0.564
α_{sfc}	0.471	0.469	0.488	0.389	0.196
α_{atm}	0.208	0.207	0.195	0.218	0.240

Table II lists the 10 hour mean, root mean-square errors (RMSE) and mean-bias errors (MBE) for reflected flux at the TOA and surface and atmospheric absorption for the four models relative to the 3D MC. These quantities are defined here as

$$\text{RMSE} = \left(\frac{1}{n} \sum_{i=1}^n \{ [x_{\text{approx}}(i) - x_{\text{MC}}(i)] S_{\odot} \mu_0(i) \}^2 \right)^{1/2} \quad (8a)$$

and

$$\text{MBE} = \frac{1}{n} \sum_{i=1}^n [x_{\text{approx}}(i) - x_{\text{MC}}(i)] S_{\odot} \mu_0(i), \quad (8b)$$

where n ($=120$) is the number of snapshots, S_{\odot} is the time-dependent solar constant, and x_{approx} and x_{MC} correspond to values in Fig. 3 for the approximate models and the 3D MC, respectively. For the ICA, MBEs are less than 5 W m^{-2} and errors are split evenly between random and bias.

For the most part, the GW TSA performs extremely well, especially for the important high Sun region. Errors for α_{toa} and α_{sfc} are typically less than 0.05 (their 10 hour mean MBEs are just -3 and 15 W m^{-2}) while those for atmospheric absorptance α_{atm} are typically less than 0.02 though there is an overwhelming tendency to underestimate. Indeed, Table I shows that relative to the ICA, the GW TSA's 10 hour mean values are in error by less than 5%. The underestimation of α_{toa} and α_{sfc} near 0800 appears to be due to excessive reduction of β below 4 km. Conversely, the overestimation of α_{toa} near 0700 and 1700 seems to stem from little reduction of β near 11 km. It is likely that both these errors are tied to the crude way in which cloud overlap is handled. While more sophisticated means of dealing with cloud overlap may eventually find their way into later incarnations of the GW TSA [per. comm., J. Bergman, 1998], it is difficult to see at this stage how these errors could be overcome in the midst of an LSM simulation given uncertainties regarding overlap rates and the potentially large radiative impact of different overlap assumptions.⁵ In fact, as Figure 3 and the Tables show, the PPH (perfect) model performs quite well given its total neglect of horizontal variability. This suggests that a fair fraction of the overall variability of cloud is captured by the implicit horizontal variability set-up by proper overlapping of PPH clouds.

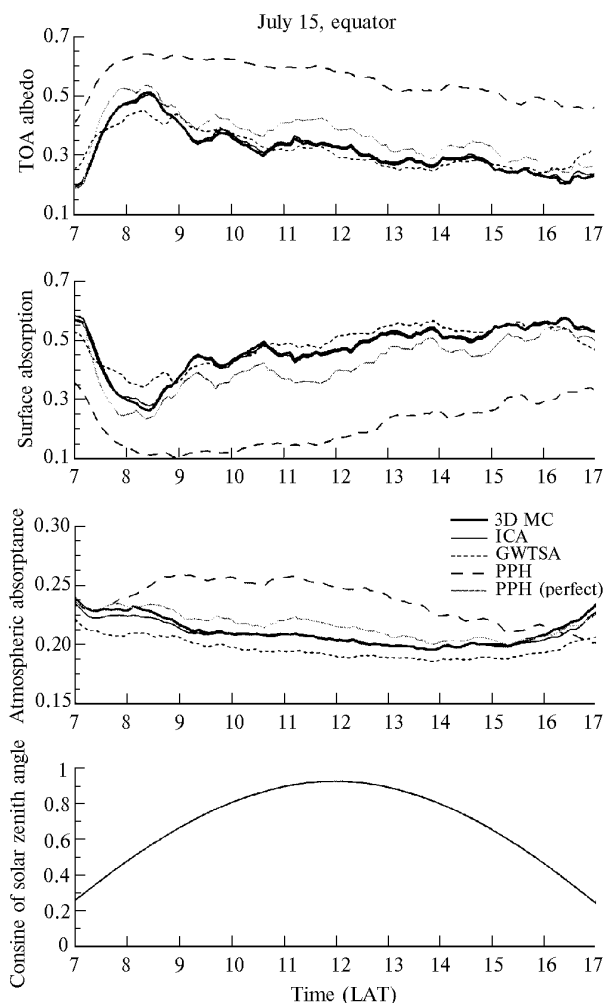


FIG. 3. Domain-averaged TOA albedo, surface absorptance, atmospheric absorptance, and μ_0 as functions of time for the Monte Carlo (3D MC), independent column approximation (ICA), gamma-weighted two-stream approximation (GW TSA), standard plane-parallel, homogeneous (PPH) two-stream, and the PPH model with perfect account of cloud overlap [PPH (perfect)].

TABLE II. Mean-bias errors (MBE) and root mean-square errors (RMSE) as defined in Eq. (8) for the four sets of model results shown on Fig. 3 relative to corresponding 3D MC values. $\text{MBE} > 0$ implies overestimation. RMSE values are in parentheses. Values are in W m^{-2} .

	ICA	GW TSA	PPH (perfect)	PPH
reflected at TOA	5.1 (7.4)	-2.9 (24.8)	66.2 (73.3)	221.3 (237.3)
absorbed at surface	-3.8 (7.6)	14.9 (30.3)	-75.0 (84.6)	-250.6 (272.3)
absorbed in atmosphere	-1.2 (2.0)	-12.0 (12.4)	8.9 (12.1)	29.3 (36.8)

As expected, the standard PPH model has difficulty right from the start. On the 10 hour mean basis, it overestimates α_{toa} , by 75% due to both outright omission of horizontal variability and the assumption of random overlapping cloud (total decorrelation of the optical and radiation fields¹⁶). As

listed in Table II, this translates to a bias error of over 200 W m^{-2} (see Ref. 5). The relative error in α_{sfc} is even more pronounced and had this simulation been over land, where cloud development would have been tied much to surface solar heating, presumably the cloud lifecycle would have been altered greatly.

The PPH model overestimates α_{atm} systematically by about 15% (MBE of $\sim 30 \text{ W m}^{-2}$) for the 10 hour mean because PPH clouds are flat, extensive sheets which are reluctant to relinquish photons once trapped within. In the other models, these clouds are either shielded to a great extent by clouds aloft, or are highly variable with no shortage of tenuous tunnels through which photons are channelled freely thereby ameliorating the number of scattering events.

Figure 4 shows profiles of 10 hour mean atmospheric

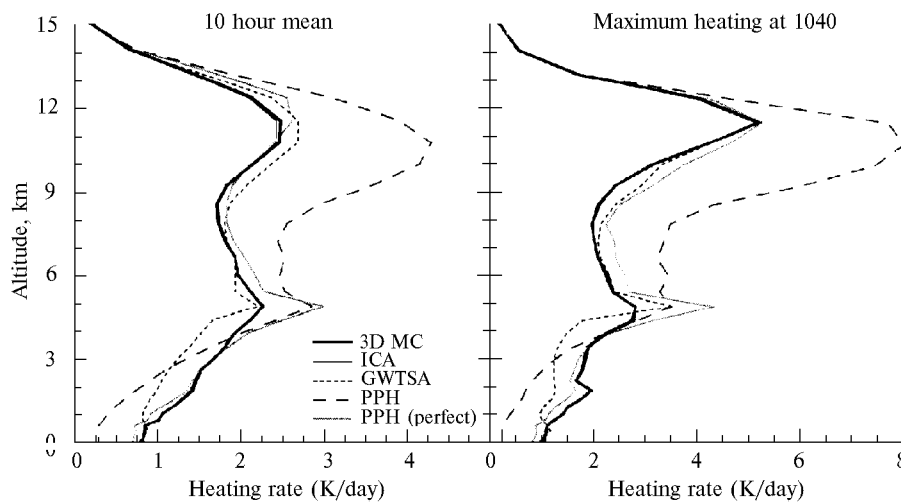


FIG. 4. Domain-averaged heating rate profiles for the Monte Carlo (3D MC), independent column approximation (ICA), gamma-weighted two-stream approximation (GWTSA), standard plane-parallel, homogeneous (PPH) two-stream, and the PPH model with perfect account of cloud overlap [PPH (perfect)]. Profiles on the left are 10 hour means while those on the right are for 1040 when the maximum values were observed.

On the other hand, the PPH model shows simply too much heating above 4 km all the time. Below 4 km there is a systematic underestimation of heating due to excessive depletion of radiation primarily through reflection by clouds aloft. The HR profile for PPH (perfect) resembles closely that for the GWTSA except near 5 km: thin cloudtops at this altitude are made too dense by the spreading out of dense convective cores. The ICA profile, however, is almost indistinguishable from that of the 3D MC.

4. SUMMARY AND CONCLUSION

An extensive set of broadband solar radiative transfer calculations were carried out and reported on here. One hundred and twenty snapshots of an evolving tropical convective cloud system, as simulated by a 2D cloud-resolving model,¹⁰ were used to initialize a Monte Carlo photon transport algorithm. Model domain size was 514 km by 18 km and the simulation spanned 10 hours with snapshots saved every 5 minutes. Cloud droplets, ice crystals, rain, snow, and graupel were considered with optical properties following Refs. 9 and 10. Nongray gaseous absorption was parametrized using the correlated- k distribution method.⁸ Domain-average profiles of cloud fraction and mean cloud extinction coefficient β were passed to two 1D radiation models,

heating rates (HRs) for all five models. Also shown are profiles for the snapshot containing the largest HRs. Clearly, the profiles for the GWTSA and the PPH (perfect) resemble that of the MC to much greater extents than does the PPH. The obvious errors committed by the GWTSA are excessive heating near 10 km (though not at 1040), and too little heating between 0.5 km and 4 km. Again, these errors are almost certainly tied to inappropriate account of cloud overlap and subsequent impacts on reductions to β .

the first of which was the regular plane-parallel, homogeneous (PPH) two-stream approximation. The other was the gamma-weight two-stream approximation^{2,15} (GWTSA) which made additional use of the mean logarithm of condensed water mixing ratios to describe unresolved horizontal fluctuations in β .

In concert with Barker et al.'s results,⁵ the PPH model exhibits biases in 10 hour mean TOA reflectance and surface irradiance in excess of $\pm 200 \text{ W m}^{-2}$. Correspondingly, it overestimates atmospheric absorptance by $\sim 30 \text{ W m}^{-2}$. Based on these results, it is difficult to see how an LSM whose solar radiative transfer is based on PPH theory (i.e., virtually all LSMs) would be able to get both tropical atmospheric hydrologic and radiation budgets correct at the same time. This statement underlies the motivation for one branch of the revived InterComparison of Radiation Codes for Climate Models (ICRCCM)⁷ (see <http://reef.atmos.colostate.edu/icrccm/icrccm.html> for more information). Moreover, it was demonstrated that roughly 70% of the PPH biases for boundary fluxes can be closed when clouds are treated as PPH yet their overlapping structure across the domain is accounted for perfectly.

The version of the GWTSA used here, which is basically the same as that presented by Oreopoulos and

Barker,¹⁵ reduces PPH biases for boundary fluxes by an order of magnitude, and reduces the atmospheric absorptance error by a factor of ~5. These improvements, however, come with a cost for in an LSM simulation, the GW TSA will require the mean logarithm of cloud mixing ratio and about twice as much CPU time as the PPH model. Presumably though, additional CPU time would be required by a PPH algorithm that properly addresses cloud overlap only. All in all, it is felt that in this highly demanding experiment, the GW TSA performed extremely well.

ACKNOWLEDGMENTS

We are thankful to Bruce Wielicki (NASA-Langley) for making computer time available. HWB was supported partially by DOE ARM grant DE-FG02-97ER2361 and QF was supported under DOE ARM grant DE-FG02-97ER62363.

REFERENCES

1. H.W. Barker, "Solar radiative fluxes for realistic extended broken cloud fields above reflecting surfaces" Ph.D. Thesis, McMaster Univ., (1991) 257 pp.
2. H.W. Barker, *J. Atmos. Sci.* **53**, 2289–2303 (1996).
3. H.W. Barker, B.A. Wielicki, and L. Parker, *J. Atmos. Sci.* **53**, 2304–2316 (1996).
4. H.W. Barker, J.-J. Ivlorrette, and G.D. Alexander, *Quart. J. Roy. Meteorol. Soc.* **124**, 1245–1271 (1998).
5. H.W. Barker, G.L. Stephens, and Q. Fu, *Quart. J. Roy. Meteorol. Soc.* (in press).
6. R.F. Cahalan, W. Ridgway, W.J. Wiscombe, T.L. Bell, and J.B. Snider, *J. Atmos. Sci.* **51**, 2434–2455 (1994).
7. Y. Fouquart, B. Bonnel, and V. Ramaswamy, *J. Geophys. Res.* **96**, 8955–8968 (1991).
8. Q. Fu and K.-N. Liou, *J. Atmos. Sci.* **49**, 2139–2156 (1992).
9. Q. Fu and K.-N. Liou, *J. Atmos. Sci.* **50**, 2008–2025 (1993).
10. Q. Fu, S.K. Krueger, and K.-N. Liou, *J. Atmos. Sci.* **52**, 1310–1328 (1995).
11. Q. Fu, M. Cribb, H.W. Barker, S.K. Krueger, and A. Grossman, *J. Atmos. Sci.* (1999) (in press).
12. L.C. Henyey and J.L. Greenstein, *Astrophys. J.* **93**, 70–83 (1941).
13. K.-N. Liou, *Radiation and Cloud Processes in the Atmosphere* (Oxford University Press, New York, 1992) 487 pp.
14. R.A. McClatchey, R.W. Fenn, J.E.A. Selby, F.E. Volz, and J.S. Garing, *Optical Properties of the Atmosphere*. 3rd ed., AFCRL-72-0497, (1972), 108 pp, [NTIS N7318412].
15. L. Oreopoulos, and H.W. Barker, *Quart. J. Roy. Meteorol. Soc.* (in press).
16. G.L. Stephens, *J. Atmos. Sci.* **45**, 1837–1848.6074 (1988).
17. W.G. Zdunkowski, R.M. Welch, and G. Korb, *Beitr. Phys. Atmos.* **53**, 147–166 (1980).
18. V.E. Zuev and G.A. Titov, *J. Atmos. Sci.* **52**, 176–190 (1995).